The Wavenumber-Phase Velocity Representation for the Turbulent Wall-Pressure Spectrum

Ronald L. Panton
Mechanical Engineering Department,
University of Texas,
Austin, TX 78712
Fellow ASME

Gilles Robert
Laboratorie de Mecanique des
Fluids et d'Acoustique,
Ecole Centrale de Lyon,
69131 Ecully Cedex, France

Wall-pressure fluctuations can be represented by a spectrum level that is a function of flow-direction wavenumber and frequnecy, $\Phi(k_1, \omega)$. In the theory developed herein the frequency is replaced by a phase speed; $\omega = ck_1$. At low wavenumbers the spectrum is a universal function if nondimensionalized by the friction velocity u^* and the boundary layer thickness δ, while at high wavenumbers another universal function holds if nondimensionalized by u^* and viscosity ν. The theory predicts that at moderate wavenumbers the spectrum must be of the form $\Phi^+(k_1^+, \omega^+ = c^+k_1^+) = k_1^+ - 2P^+(\Delta c^+)$ where $P^+(\Delta c^+)$ is a universal function. Here Δc^+ is the difference between the phase speed and the speed for which the maximum of Φ^+ occurs. Similar laws exist in outer variables. New measurements of the wall-pressure are given for a large Reynolds number range; $45{,}000 < Re = U_0\delta/\nu < 113{,}000$. The scaling laws described above were tested with the experimental results and found to be valid. An experimentally determined curve for $P^+(\Delta c^+)$ is given.

Introduction

In the general situation where a boundary layer develops slowly, the flow only depends on the local properties; the layer thickness, friction velocity, fluid density, pressure gradient, and the characteristic Mach number and Reynolds number of the flow. This paper deals with incompressible flow where the Mach number is nearly zero. As in the general theory of turbulent boundary layers the development is organized as the limiting behavior for high Reynolds numbers. Although the data we will present are for zero-pressure gradients, the theory is also applicable to flows with pressure gradients.

It is well-known that turbulent boundary layers have two distinctively different layers; the outer inviscid layer and the inner wall layer. These layers are not mutually exclusive but have a region of overlap, the "log region." The extent of the overlap region increases directly with the Reynolds number. Because the wall pressure is influenced by turbulent motions from throughout the boundary layer, changes in boundary layer overlap structure are reflected by changes in the spectrum. In this paper, we develop a theory that accounts for the expansion of the frequency range in a rational way.

Over the last thirty years numerous measurements of the wall-pressure field have been made. Even though approaches exist which seek to characterize the signature of wall pressure from coherent turbulent structures (Dinkelacker, 1977; Wilczynski and Casarella, 1993) experimental studies generally concern the statistical description of the wall-pressure field. Results for $R_{pp}(\xi, \zeta, \tau)$ are presented in physical and temporal space (for example, Willmarth, 1975) and Panton, 1980). Related quantities have been studied in physical and frequency space, $S_{pp}(\xi, \zeta, \omega)$, by among others, Bull (1967), Blake (1970), Willmarth (1970), for aerodynamic boundary layers, and by Carey (1967), Bakewell (1968), and Benarrous (1979) for hydrodynamic boundary layers. Fourier transforming the results obtained in physical space (Wills, 1970; Karangelen et al., 1991); Manoha, 1991) gives one access to a continuous representation of the cross-spectrum in $k-\omega$ space.

Theory

A physical characteristic of turbulent wall layers is that the fluctuations, which have a small characteristic velocity, are convected with a much larger velocity. The crudest approximation is that the convection velocity is a constant fraction of the free-stream velocity. A much better approximation is that the convection velocity is approximately the local mean velocity. The physical process of convection is emphasized by introducing a phase velocity defined by

$$c = \omega/k_1 \tag{1}$$

With this substitution the spectrum function $\Phi(k_1, \omega)$ can be given as a function of k_1, and c.

$$\Phi = (k_1, ck_1) \tag{2}$$

(Wills (1970) used this approach to separated acoustic noise from his measurements.) The physical picture is that the pressure fluctuations are primarily the result of superimposed components of wavenumber k_1, being convected at a speed c over the wall. At a specific point on the wall it is expected that turbulent fluctuations of small scale convected at a low speed will produce the same frequency as a large fluctuation con-

Contributed by the Fluids Engineering Division for publication in the JOURNAL OF FLUIDS ENGINEERING. Manuscript received by the Fluids Engineering Division January 25, 1993; revised manuscript received September 29, 1993. Associate Technical Editor: D. M. Bushnell.

vected at a high speed. By using c and k_1 as independent variables the contributions of different size eddys to the same frequency are separated.

It is a fact that the extent of influence of a turbulent fluctuation is proportional to its size. The largest fluctuations have a spatial scale about the size of the boundary layer thickness, while the smallest scales are related to the thickness of the viscous sublayer. Thus, a small eddy that is in the outer layer is not felt on the wall. This is particularly true as the Reynolds number becomes high and the outer layer is large compared to the inner layer. If it is valid that the highest wavenumber portion of the spectrum comes only from the inner layer then the proper nondimensional variables are scaled with the inner scales u_* and ν, that is

$$\Phi^+ = \frac{\Phi(k_1, \omega)}{\rho^2 \nu^2 u_*}, \quad k_1^+ = \frac{k_1 \nu}{u_*}, \quad c^+ = \frac{c}{u_*} \tag{3}$$

In this form the spectrum Φ^+ should be nearly independent of the Reynolds number in the region of high k_1. Moreover, this portion of the spectrum should not be influenced greatly by an external pressure gradient.

At the other end of the spectrum, the largest turbulent eddys exist only in the outer layer and have a size scaled by the boundary layer thickness δ. The intensity of fluctuation in these eddys also scales with u^*. The appropriate outer scaling (the use of u^* and δ for scaling the frequency spectrum was proposed long ago and has been experimentally confirmed by Farabee and Casarella, 1991) is

$$\Sigma = \frac{\Phi(k_1, \omega)}{\rho^2 u_*^3 \delta^2}, \quad K_1 = k_1 \delta, \quad C = \frac{c - U_\infty}{u^*} \tag{4}$$

At low wavenumbers this form for Σ should be roughly independent of the Reynolds number, however, it will be sensitive to the pressure gradient. An important assumption is that the phase velocity is expressed as a defect law; an analogy with the mean velocity profile where it is known to be the correct form.

The ratio of outer and inner scales is the Reynolds number

$$\mathrm{Re}_* = \frac{u_* \delta}{\nu} \tag{5}$$

Inner and outer spectrum variables, defined above, are simply related through this Reynolds number. The relations are

$$\Sigma = \Phi^+ \mathrm{Re}_*^{-2}, \quad K_1 = k_1^+ \mathrm{Re}_*, \quad C = c^+ - U_\infty / u_* \tag{6}$$

It should be noted that U_∞ / u_* is a function of the Reynolds number.

Next, we consider the ridge in the $k_1 - c$ plane where Φ has a local maximum for constant wavenumber ($\partial\Phi$, $\partial c = 0$). The values along the ridge are noted by the subscript max and the location is the curve $c^+_{\max} = c^+_{\max}(k_1^+)$.

$$\Sigma_{\max}(K_1) = \Sigma(K_1, K_1\, C_{\max})$$

$$\Phi^+_{\max}(k_1^+) = \Phi^+(k_1^+, c^+_{\max} k_1^+) \tag{7}$$

The curve $c^+_{\max}$ can be considered as the convective velocity of the pressure fluctuations. As with the complete spectra these maxima functions are independent of Reynolds number in the inner and outer scaling at high and low wavenumbers, respectively. Of interest in the current paper is the overlap convective law given by Panton and Linebarger (1974).

$$c^+_{\max} = \frac{c_{\max}}{u_*} = -\frac{1}{\kappa} \ln(k_1^+) + C \tag{8}$$

The constants here are the same as those in the mean velocity law (note that conversion of Eq. (8)) from k_1^+ to K_1 is accomplished using the friction law;

$$\frac{U_\infty}{u_*} = \frac{1}{\kappa} \ln(\mathrm{Re}_*) + C + \frac{2\Pi}{\kappa}.$$

Assume that there is an overlap region in $\Phi_{\max}$ as a function of k_1 where both inner and outer scaling are valid. That is, there is a region of intermediate wavenumbers where both expressions in Eq. (7) are valid

$$\Sigma_{\max} = \Phi^+_{\max} \mathrm{Re}_*^{-2} \tag{9}$$

Since this is a finite region we may differentiate Eq. (9) with respect to K_1 to obtain

$$\frac{d\,\Sigma_{\max}}{dK_1} = \frac{d(\Phi^+_{\max} \mathrm{Re}_*^{-2})}{dk_1^+} \frac{dk_1^+}{dK_1}$$

Using the relation $K_1 = k_1^+ \mathrm{Re}_*$, separating variables, and considering K_1 and k_1^+ to be independent (for fixed K_1, Re_* could be changed) leads to

$$K_1^3 \frac{d\,\Sigma_{\max}}{dK_1} = (k_1^+)^3 \frac{d\Phi^+_{\max}}{dk_1^+} = \text{Constant} = A' \tag{10}$$

One of the two differential equations that result is

$$d\,\Sigma_{\max} = A' K_1^{-3}\, dK_1$$

Thus, in the range of wavenumbers where there is an overlap, the behavior of the maximum values must be

$$\Sigma_{\max} = A K_1^{-2} + C_1 \tag{10a}$$

Similar arguments produce the inner form of this relation

Nomenclature

c = phase speed
$c_{\max}$ = convection velocity
f = frequency
k_1 = streamwise wavenumber
p = pressure fluctuation
Re_* = Reynolds number $u_* \delta / \nu$
$R_{pp}(\xi, \zeta, \tau)$ = cross-correlation function
$S_{pp}(f)$ = wall-pressure power spectral density
$S_{pp}(\omega)$ = wall-pressure spec-trum: $4\pi S_{pp}(\omega) = S_{pp}(f)$
$S_{pp}(\xi, \zeta, \omega)$ = wall-pressure cross-spectrum
U_∞ = free-stream velocity
u_* = friction velocity
α = coefficient for streamwise decay of coherence
δ^* = displacement thickness
δ = boundary layer thickness
ρ = density
$\Phi(k_1, k_2, \omega)$ = wavenumber and frequency cross-spectrum
$\Phi(k_1, \omega)$ = integrated wavenumber spectrum
ν = kinematic viscosity
τ = time delay
τ_0 = mean wall shear stress ($\tau_0 = \rho u^{*2}$)
ξ, ζ = streamwise and transverse separation distance
ω = angular frequency, $2\pi f$
$P^+(c^+, k_1^+)$ = spectrum function
$R_{pp}(\xi, \zeta, \tau)$ = $p(x, z, t) \cdot p(x+\xi, z+\zeta, t+\tau)$
$S_{pp}(\xi, \zeta, \omega)$ = $1/2\pi \int R_{pp}(\xi, \zeta, \tau) \cdot \exp(-i\omega\tau)$ $d\xi\, d\zeta\, d\tau$—
$\Phi(k_1, k_3, \omega)$ = $1/8\pi^3 \int R_{pp}(\xi, \zeta, \tau) \cdot \exp(i(k_1\xi + k_3\xi - \omega\tau))d\xi\, d\zeta\, d\tau$
$\Phi(k_1, \omega)$ = $\int \Phi(k_1, k_3, \omega) dk_3$

$$\Phi^+_{max} = A\ k_1^{+-2} + C_2 \qquad (10b)$$

Back substitution into Eq. (9) shows that the constants are zero. Equations (10) were previously given by Panton (1990).

The essential mathematical element of the argument above is that a function of the single variable, k_1, has an overlap region which expands with Reynolds number. Any other mathematical property of the spectra where c is eliminated to leave only the independent variable k_1 can be similarly treated. Here we extend the argument to prove that the spectra in the overlap region must also have a universal shape. Consider the integral below over c^+ with k_1^+ as a parameter

$$I^+(k_1^+) \equiv \int \Phi + (k_1^+, c^+ k_1^+) d(c^+ k_1^+) \qquad (11a)$$
$$k_1^+ = \text{constant}$$

Transforming the integral into outer variables yields

$$I^+(k_1^+) = \text{Re}^* \int \Sigma(K_1, CK_1)\, d(CK_1) \equiv \text{Re}^* \mathbf{I}(K_1) \qquad (11b)$$

Applying the same overlap argument as above to the functions $I^+(k_1^+)$ and $\mathbf{I}(K_1)$ shows that we should expect a range of moderate wavenumbers where the integrals must have the following trends

$$I^+(k_1^+) = B\ k_1^{+-1} \qquad \mathbf{I}(K_1) = B\ K_1^{-1} \qquad (12)$$

Next, consider that the expressions in Eq. (12) can be solved for the constant B

$$B = k_1^+ I^+(k_1^+) = \int k_1^{+2}\, \Phi^+(k_1^+, c^+ k_1^+)\, dc^+ \qquad (13)$$

Let the integrand be denoted by P^+

$$P^+(c_1^+, k_1^+) \equiv k_1^{+2} \Phi^+(k_1^+, c^+\ k_1^+) \qquad (14)$$

Consider P^+ as a function of c^+ with k_1 as a parameter. Furthermore, note that there is no change in the level of P^+ when it is expressed in outer variables.

$$P^+(c^+, k_1^+) = k_1^{+2}\Phi^+ = \left(\frac{K_1}{\text{Re}^*}\right)^2 \Sigma\ \text{Re}^{*2}$$
$$= K_1^2 \Sigma = \mathbf{P}(C, K_1) \qquad (15)$$

We will call P^+ or P the *spectrum function*.

For constant wavenumber the peaks of the P^+ curves can be lined up by introducing the variable

$$\Delta c^+ = c^+ - c^+_{max}(k_1) \qquad (16)$$

In the overlap range c^+_{max} is given by Eq. (10). Likewise, the outer representation should be based on the defect velocity

$$\Delta C \equiv C - C_{max} = \Delta c + \qquad (17)$$

Equations (15) and (17) imply that any statement about $P^+(c^+, k_1^+)$ also applies to $P(C, K_1)$.

Next we will show that P^+ has a universal form, that is $P^+(c^+, k_1^+) = P^+(\Delta c^+)$ for any k_1^+ is in the overlap region. To prove this consider a new integral from the maximum c^+_{max} to an arbitrary point $c^+_{max} + \Delta c^+$

$$I_2^+(k_1^+; \Delta c^+) = \int_{c^+_{max}}^{c^+_{max} + \Delta c+} P^+(c^+, k_1^+)\, dc^+$$

Since $P^+(c^+, k_1^+) = P(C, K_1)$, Eq. (15), and $\Delta C = \Delta c^+$, Eq. (17), the value of this integral is unchanged when it is transformed into outer variables, that is

$$I_2^+(k_1^+; \Delta c^+) = \int_{C_{max}}^{C_{max} + \Delta C} \mathbf{P}(C, K_1)\, dC = I_2(K_1; \Delta C) \qquad (18)$$

Therefore, the overlap arguments can be applied to show that I_2^+ is constant (for fixed Δc^+) over the range of overlap wavenumbers. Equally as important is the fact that the argument is good for any choice of $\Delta c^+ = \Delta C$.

Figure 1 shows the integral for a certain value of Δc^+ for two different wavenumbers. Assume the opposite of what we desire to prove; namely, that the curves for two different overlap wavenumbers are distinct as shown. Since the integrals are equal by Eq. (18) there must be a crossover point between c^+_{max} and $c^+_{max} + \Delta c^+$. If this were true we could immediately choose the crossover point as a new $\Delta c+$ and the integrals to this new value would be different. This contradicts the known fact in Eq. (18), hence the curves $P^+(\Delta c^+) = \mathbf{P}(\Delta C)$ must be identical (universal) for all k_1^+ in the overlap region.

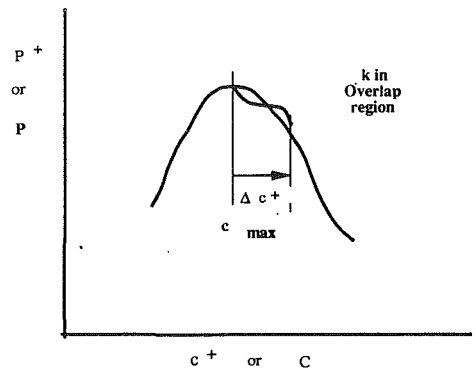

Fig. 1 Spectrum function $P^+(c^+)$. Two curves for distinct wavenumbers.

Table 1 Boundary layer characteristics

Uo m/s	20	30	40	50	60
u_* m/s	0.826	1.18	1.56	1.9	2.19
δ m	0.0358	0.0358*	0.0359	0.0358*	0.0359
Π	0.16	0.16*	0.087	0.16*	0.27
C	5.082	5.082*	5.018	5.082*	5.52
d^+	166	238	314	385	
Re_*	1908	2725	3662	4400	5086

*Extrapolated values from 20 m/s.

As an aside we note that if one deals with the complete spectrum with zero spanwise separation $\Phi^+_{pp}(k_1^+, k_3^+ = 0, c + k_1^+)$, as opposed to the spectrum that is integrated over k_3^+, the corresponding result is $\Phi^+_{pp}(k_1^+, k_3^+ = 0, c^+ k_1^+) = k_1^{+-3} \mathbf{P}^+_{pp}(\Delta c^+_1 k_1^+)$.

We summarize the results with the following statements. For high wavenumbers the spectrum function $P^+(\Delta c^+, k_1^+)$ depends on k_1^+ but should be independent of the Reynolds number. Similarly, for low wavenumbers the outer representation $P(\Delta C, K_1)$ should be roughly independent of Reynolds number. The range of overlap wavenumbers that connects these representations expands directly with increasing Reynolds number. It has been shown that within an overlap range of wavenumbers, denoted by $K_{1\,min}$ to $k^+_{1\,max}$, the spectrum function is a universal function $P^+(\Delta c^+)$; in other words, $P^+(\Delta c^+, k_1^+)$ becomes independent of k_1^+.

Moreover, it has previously been proposed, Panton and Linebarger (1974), that the convection velocity c^+_{max} is a universal function for high wavenumbers, C_{max} is a universal function for low wavenumbers, and the overlap region is given by Eqs. (18).

Comparison with Experiments

The theory was tested by measurement made in the wind tunnel of the Acoustics Center at Ecole Centrale de Lyon. The tunnel, illustrated in Fig. 2 and described more fully in Robert (1993), was especially constructed to minimize acoustic contamination by upstream machinery and ambient noise.

The mean velocity profiles, shown in Fig. 3, were measured with a Pitot tube for three flow speeds: 20, 40, 60 m/s. These profiles were used to determine the parameters u^*, δ, and Π by the methods which are fully given by Robert (1993). The values, see Table 1, are consistent with the different laws directing the characteristics of the boundary layer at different speeds. The wake components, Π, are variable and somewhat smaller than the nominal value of 0.6. Casarella and coworkers

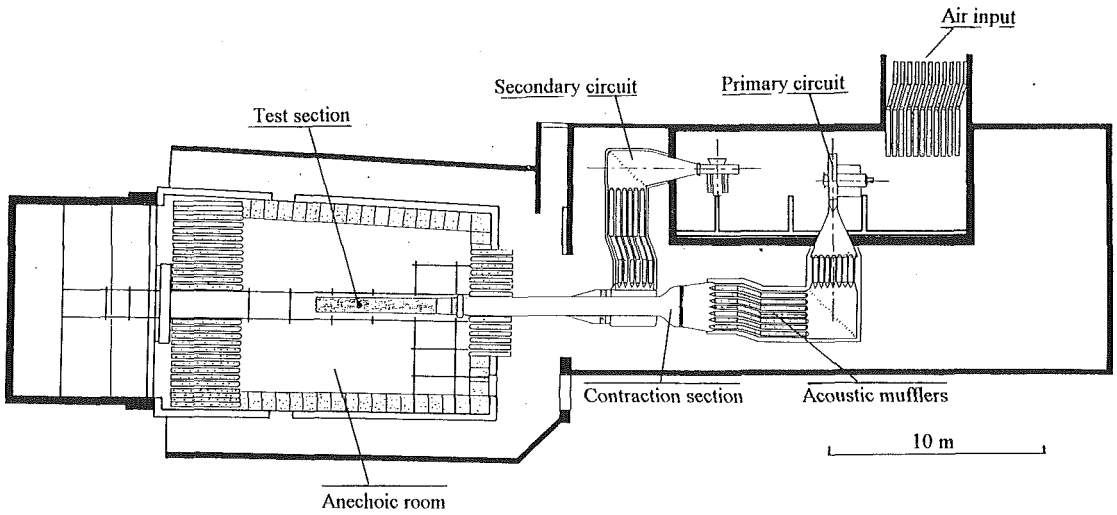

Fig. 2 The anachoic wind tunnel facility at Ecole Centrale de Lyon

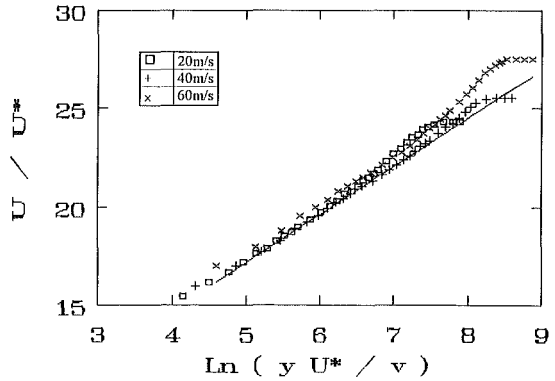

Fig. 3 Boundary layer velocity profiles. Law of the wall coordinates.

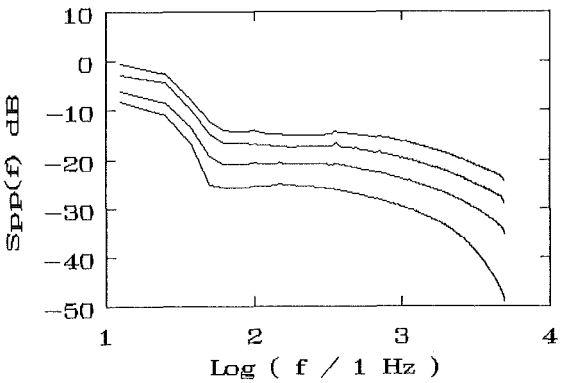

Fig. 4 Wall pressure frequency spectra in dB (ref 1 Pa^2/Hz) for 20, 30, 40, and 50 m/s. Note that the origin is shifted for each curve.

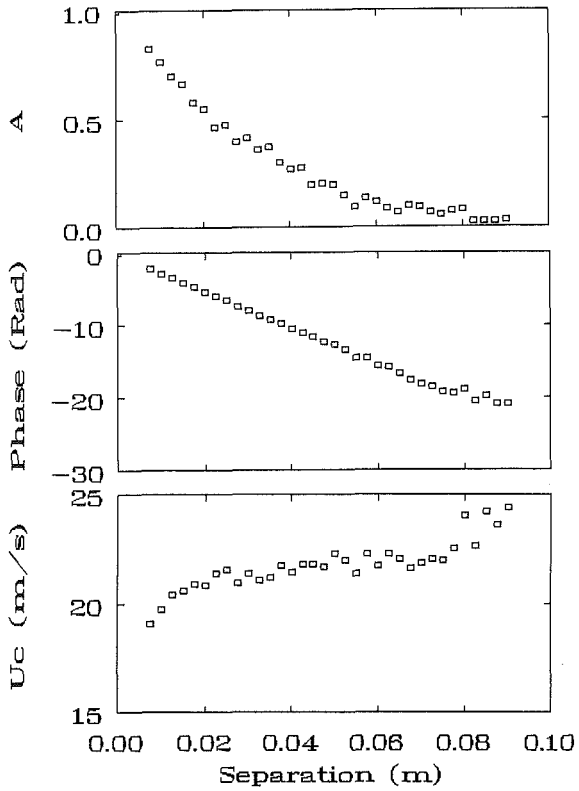

Fig. 5 Streamwise cross-spectrum of the wall pressure for $U_o = 30$ m/s and $f = 900$ Hz; (*a*) coherence function, (*b*) phase function, (*c*) convection velocity

(private communication) have noted that the method of tripping has a large and longlasting effect on this value.

The frequency spectra measurements are presented for the four velocities in Fig. 4. In this figure one can observe some strong energetic levels at very low frequencies. These levels comes from stationary acoustic waves that occur in the test section between the upstream convergent and the exit section. In what follows we will limit the displays to frequencies above 50 Hz. The spectra levels obtained in the present study are roughly 1dB lower than those of Farabee and Casarella (1991).

A more precise description of the wall-pressure field is obtained with the cross-spectrum $S_{pp}(\xi, \zeta, \omega)$. Below we discuss only the behavior with respect to ξ. In general, the cross-spectrum is a complex function that is often represented by the coherence function $A(\xi, \omega) = |S_{pp}(\xi, 0, \omega)|/(S_{p1}(\omega) S_{p2}(\omega))^{0.5}$ together with a phase function $\Theta(\xi, \omega)$. The coherence expresses the decreasing activity of the pressure field associated with the ω frequency when it is convected over a distance ξ. A (different) convection velocity is obtained from $U_c(\xi, \omega) = \omega\xi/\Theta(\xi, \omega)$. A typical example of the evolution of these three functions is shown in Fig. 5. At a given frequency, the coherence function shows a nearly exponential decrease with ξ while the phase increases almost, but not quite, linearly. The departure of the phase from linearity is easier to see in the convection velocity which increases slightly with the separation.

For a given frequency the cross-spectrum $\Phi(k_1, \omega)$ was ob-

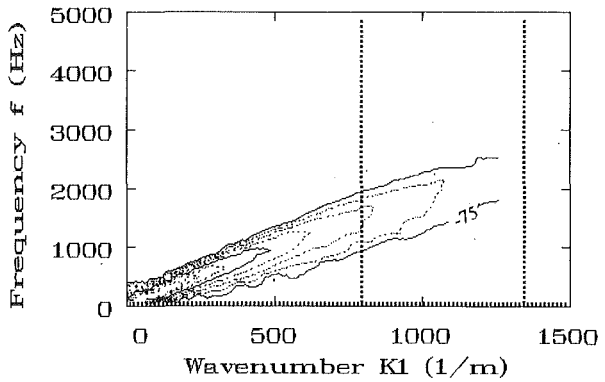

Fig. 6 Contour plot of streamwise wave number frequency spectrum of wall pressure in dB (ref 1 Pa^2 m/Hz) with increments of 2.5 dB for $U_o = 20$ m/s. Frequency (50 Hz) and wave number limits (1 db and 3db loss from microphone spatial sensitivity) are given by dashed line.

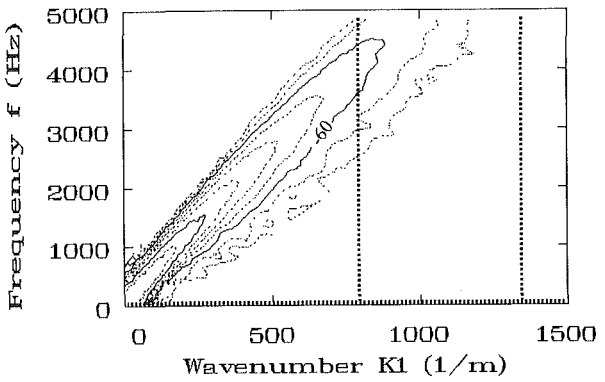

Fig. 7 Contour plot of streamwise wave number frequency spectrum of wall pressure in dB (ref 1 Pa2 m/Hz) with increments of 2.5 dB for $U_o = 20$ m/s.

tained by a fast Fourier Transform over the space variable ξ of the cross-spectrum $S_{pp}(\xi, 0, \omega)$. A typical wavenumber cross-spectrum presents a principal peak that characterizes the convected nature of the wall-pressure field. The evolution of the convection peak is presented as a function of frequency for the two extreme Reynolds numbers in Figs. 6 and 7. Two types of limit lines are shown on the figures; one for the 50Hz acoustic standing waves mentioned earlier and the second corresponding to two estimates for the transducer resolution. The estimates were made considering a one db and three db loss of response for a circular diaphragm with a radius 80 percent of the microphone radius.

The increase of the flow velocity, and thus the convection velocities, manifests itself in the straightening of the convection contours towards the frequency axis. As Wills (1970) and Choi and Moin (1990) have observed, the convection ridge has a tendency to broaden when the frequency rises. This broadening is induced by the reduction of the correlation lengths at high frequencies. The ridge presents a strong asymmetry with an abrupt fall of level toward the low wavenumbers. This behavior is equally observable in the results of Willis and Choi and Moin but less so than in those of Karangelen et al. (1991). This asymmetry cannot come from the FFT process on the cross-spectrum modulus because it only acts grossly and in a symmetrical fashion on the width of the convection peak. It comes instead from the nonlinearity of the phase Θ as a function of the separation. That is to say the evolution of the convection velocity with the separation. A constant convection velocity, that is Θ a linear function, would only induce a symmetrical convection peak centered on ω/U_c in the wavenumber space.

The experimental results were reprocessed into the form $\mathbf{P}(\Delta C, K_1)$ and contour plots for wind tunnel speeds of 20,

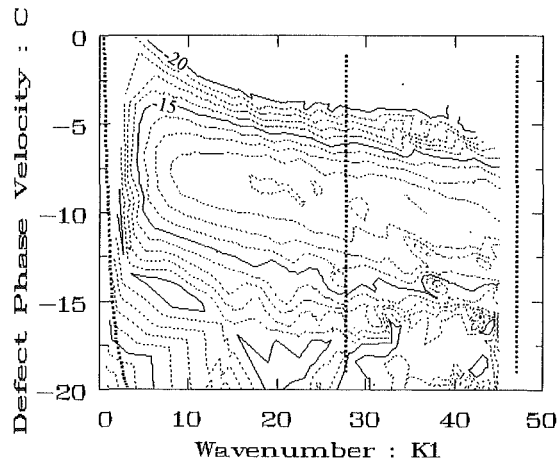

Fig. 8 Spectrum function $P(K, C)$. Level in dB (5 dB between solid lines) $U_o = 20$ m/s, $Re^* = 1908$. Frequency and wave number limits given by dashed line.

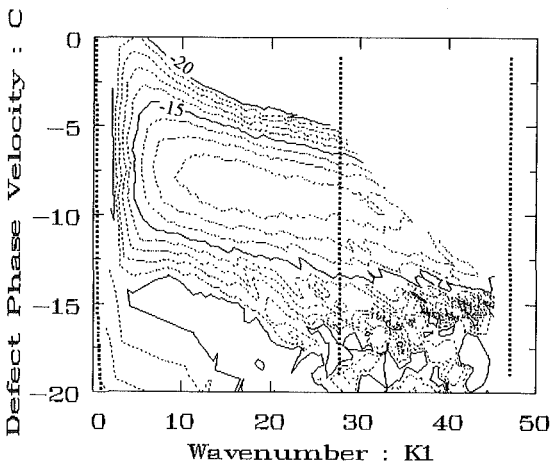

Fig. 9 Spectrum function $P(K, C)$. Level in dB (5 dB between solid lines) $U_o = 50$ m/s, $Re^* = 4400$. Frequency and wave number limits given by dashed line.

30, 40, and 50 m/s, $Re^* = 1900$ to 4500, and plotted in contour maps. The extreme cases are given in Figs. 8 and 9. Note that all of the data presented are made dimensionless by boundary layer parameters and not by the rms of the signals. The limit lines for acoustic interference and transducer resolution are again shown.

The overlap region where $\mathbf{P}(\Delta C, K_1)$ is only a function of ΔC is also evident. This is seen more accurately in Figs. 10 through 12 where cuts at constant wavenumber for the different Reynolds number are plotted. At $K_1 = 10$ the overlap region has not been reached as the peak of the curves are noticeably lower than those of the other figures. Comparison of the remaining curves with each other shows no significant difference. For reference a curve fit to the data (from $K_1 = 20$, and 30) is plotted. The equation that resulted is

$$10 \text{ Log } P = A + B\Delta C + C(\Delta C)^2 + D(\Delta C)^3 + E(\Delta C)^4 + F(\Delta C)^5 \quad (19)$$

$$A = -11.09,\ B = 0.05333,\ C = -0.3851,$$

$$D = -0.03458,\ E = 0.005006,\ F = 0.0007544$$

The free-stream speed, $C = 0$, is an effective maximum for the phase speed.

The drop-off in the spectrum at very low wavenumbers is shown in Fig. 13. Here cuts of the spectrum function are made at constant wavenumbers and the data from the two extreme Reynolds number grouped on a single graph. The similarity

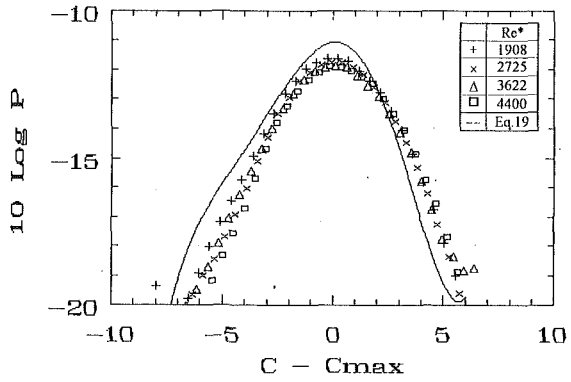

Fig. 10 Spectrum function at $K_1 = 10$ for all Re*

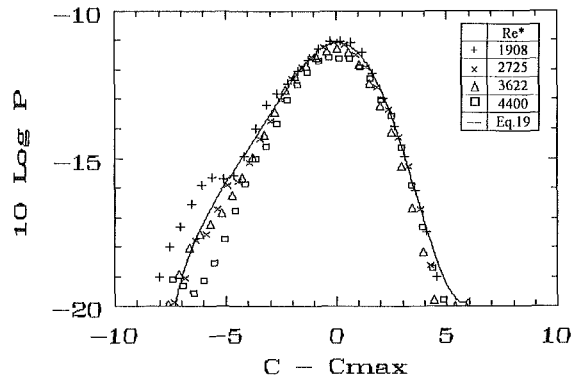

Fig. 11 Spectrum function at $K_1 = 20$ for Re*

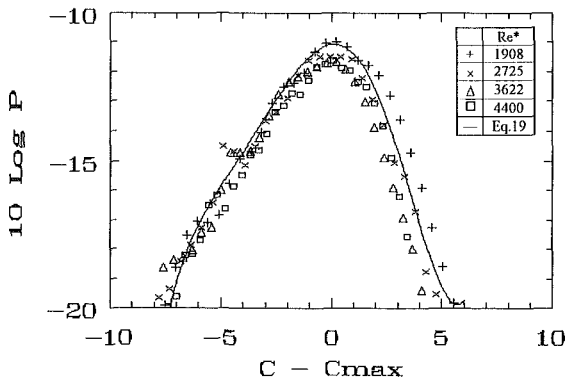

Fig. 12 Spectrum function at $K_1 = 30$ for all Re*

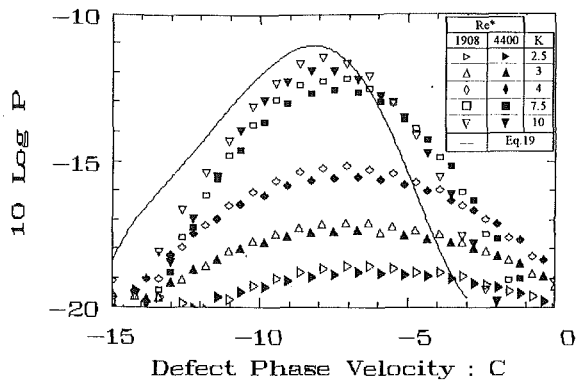

Fig. 13 Spectrum function for low wavenumbers at different K for Re* = 1908 and 4400.

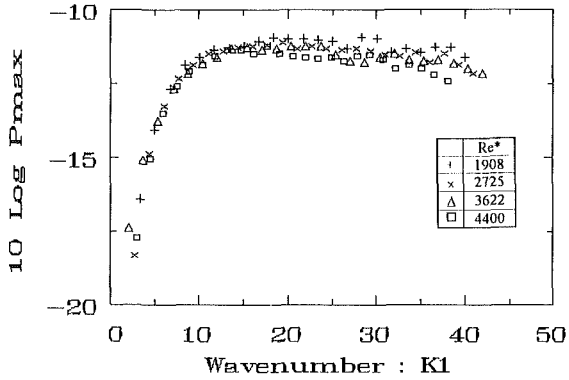

Fig. 14 Maximum of spectrum function for all Re*

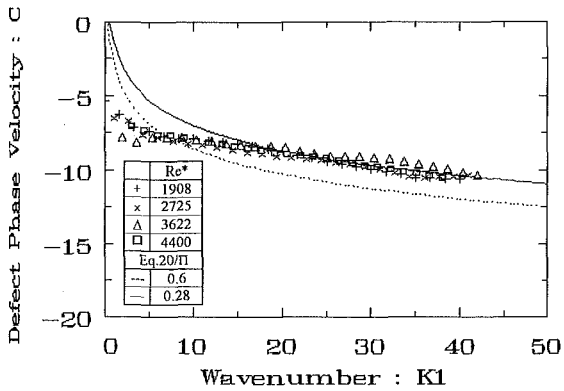

Fig. 15 Convective velocity

with Reynolds number is very good and confirms, at least for these values, that the low wavenumber spectrum is independent of Re* (see also Fig. 14). Theoretically these wavenumbers are sensitive to pressure gradient. As the wavenumber decreases the content at low phase velocities remains about the same, the peak decreases and moves slightly to higher velocities, and the content at high phase velocities broadens noticeably. For example, at a wavenumber of $K_1 = 4$ the curves rise rapidly from $C = 0$, essentially the free-stream velocity. Although the spectrum levels at low K_1 and high velocities are quite low the broadening is to be expected physically. It is well-known that boundary layers have potential fluctuations out to distances considerably larger than $y = \delta$. Explicit evidence of the connection between the potential fluctuations and the wall pressure has been obtained by correlating a hot wire at distances greater than δ and a wall microphone. Such data have been given by Farabee and Casarella (1991) and Panton et al. (1980).

The drop-off of the maximum values of the spectrum function is presented in Fig. 14 for all Reynolds numbers. Again the curves correlate very well. There is negligible contribution to the spectrum function (seven db down from the peak) for wavenumbers less than $K_1 = 2.5$. The value for which the level reaches a constant, 10 log $P = -11$, marks the lower end of the overlap region and is about $K_{min} = 14$ (the corresponding wavelength is $\Lambda_{min} = 0.45\ \delta$). This is a little higher than the value of $K_{min} = 6$ chosen by Karangelen et al. (1991). The data show a slight downward trend at higher wavenumbers, however, the accuracy of the calculation and scatter of the results are becoming larger so this is probably not an actual physical trend.

The convective velocities C_{max} (K_1) for all Reynolds numbers are given on Fig. 15. The different Reynolds numbers correlate very well in terms of these variables, especially when one notes that blunt contours give difficulty in obtaining C_{max} when K_1

is low. For the overlap region of wavenumbers the theoretical relation obtained by rearranging Eq. (8) is

$$C_{\max} = -\frac{1}{\kappa} \ln (K_1) - \frac{2\Pi}{\kappa} \tag{20}$$

This equation is shown on Fig. 15 for two values of the wave strength constant Π, 0.28, and 0.6. The values 0.28 is a fit to the data of the figure while 0.6 is the number most often given as typical of zero pressure gradient boundary layers. For comparison recall (Table 1) that the tested velocity profiles yielded values of 0.09 to 0.27. The fact that the detailed nature of the outer flow is very important to the low wavenumber spectrum was emphasized by Farabee and Casarella (1991) and we concur on this point.

The deviation from the overlap law, a wake law if you like, occurs toward lower values of the velocity. This is in agreement with the results presented recently in Karangelen et al. (1991) but in the opposite direction from the older data of Wills (1970). Also noted from Figs. 8 and 9 that the contours are very broad and blunt in this region. The results do not approach the free-stream as $K_1 \rightarrow 0$. This means that there are always very low wavenumber components within the boundary layer traveling at low velocities that are as important as the low wavenumber potential motions in the free-stream.

Because of transducer spatial resolution and the minimum spacing between microphones, the data do not extend to high enough wavenumbers to see the drop off in the spectrum function from viscous effects. We can guess that this begins for wavelengths about twice the buffer layer thickness. $\lambda^+ = 100$ or $k^+_{\max} = k_1 \nu / u^*]_{\max} = 0.0625$. For a Reynolds number of $\mathrm{Re}^* = 1000$ this is equivalent to $K_1 = 62$, a value beyond the range of the measurements.

Conclusions

The wall pressure fluctuations under a turbulent wall layer have been discussed in terms of a spectrum function with streamwise wavenumber k_1 and phase velocity c as variables. The conversion of the frequency into a wavenumber and phase velocity, $\omega = k_1 c$, allows a theory that postulates an overlap range of wavenumbers where both inner and outer variables are valid. The most important theoretical conclusion is that the spectrum in the overlap region is of the form $\Phi^+(k_1^+, \omega^+ = c^+ k_1^+) = (k_1^+)^{-2} P^+(\Delta c^+)$ in inner variables or $\Sigma = K_1^{-2} \mathbf{P}(\Delta C)$ in outer variables. Here $\Delta c^+ = \Delta C$ is the difference between the phase speed and the speed for which the maximum of Φ^+ occurs. Experimental data validate the overlap form and show that $\mathbf{P}(\Delta C) = P^+(\Delta c^+)$ is an asymmetric function. This representation is valid from $k_1 \delta]_{\min} = 14$ to some value of $k_1 \nu / u^*]_{\max}$ (about 0.0625?) which is too high for the experiments to resolve. The overlap convective law for $c_{\max}$ from previous theory was also verified.

For values of the wavenumber lower than $K_{\min}$ the spectrum function $\mathbf{P}(K_1, C)$ falls rapidly and is seven db down from the peak when the wavenumber is $K_1 = 2.5$. Also at low wavenumbers the spectrum funciton broadens and shows a small contribution from the potential motions as $c \rightarrow U_\infty$. At least in the range of experiments covered by the experiments, $\mathrm{Re}^* = 1000$ to 4,500 the low wavenumber convective events scale are independent of Reynolds number when scaled on outer variables including a defect phase velocity.

Acknowledgment

The first author expresses appreciation to the Rhone-Alpe Region of France for a Bourse d'Accueil and to the University of Texas for a Research Assignment.

This experimental program was sponsored by the Direction des Recherches et Etutes Techniques.

References

Bakewell, H. P., 1968, "Turbulent Wall Pressure Fluctuations on a Body of Revolution," *Journal of Acoustical Society of America*, Vol. 43, No. 6, pp. 1358-1363.

Benarrous, E., 1979, "Contribution à l'étude des fluctuations de pression pariétale sous une couche limite turbulente," Thèse No. 897, Univ. Claude Bernard, Lyon, France.

Blake, W. K., 1970, "Turbulent Boundary-Layer Wall-Pressure Fluctuations on Smooth and Rough Walls," *Journal of Fluid Mechanics*, Vol. 44, Part 4, pp. 637-660.

Blake, W. K., and Chase, D. M., 1971, "Wavenumber-Frequency Spectra of Turbulent Boundary Layer Pressure Measured by Microphone Arrays," *Journal of Acoustical Society of America*, Vol. 49, No. 3, Part 2.

Bull, M. K., 1967, "Wall-Pressure Fluctuations Associated With Subsonic Turbulent Boundary Layer Flow," *Journal of Fluid Mechanics*, Vol. 28, Part 4, pp. 719-754.

Carey, G. F., Chlupsa, J. E., and Schloemer, H. H., "Acoustic Turbulent Water-Flow Tunnel," *Journal of Acoustical Society of America*, Vol. 41, No. 2, 1967, pp. 373-379.

Choi, H., and Moin, P., 1990, "On the Space-Time Characteristics of Wall-Pressure Fluctuations," *The Physics of Fluids*, Vol A2 (8), Aug. pp. 1450-1460.

Dinkelacker, A., Hessel, M., Meier, G.E.A., and Schewe G., 1977, "Investigation of Pressure Fluctuations Beneath a Turbulent Boundary Layer by Means of an Optical Method," *The Physics of Fluids*, Vol. 20, No. 10, Part II, Oct.

Farabee, T. M., and Geib, F. E. Jr., 1976, "Measurement of Boundary Layer Pressure Fields with an Array of Pressure Transducers in a Subsonic Flow," Naval Ship Research and Development Center, Ship Acoustics Department Research and Development Report 76-0031.

Farabee, T. M., and Casarella, M. J., 1991, "Spectral Features of Wall Pressure Fluctuations Beneath Turbulent Boundary Layers," *Physics of Fluids*, Vol. 3, pp. 2410-2420.

Karangelen, C. C., Casarella, M. J., and Farabee, T. M., 1991b, "Wavenumber-Frequency Spectra of Turbulent Wall Pressure Fluctuations," ASME Winter Annual Meeting, NCA-Vol. 11/FED-Vol. 130, pp. 37-44, submitted to ASME *Journal of Vibrations and Acoustics*.

Manoha, E., 1991, "Wall Pressure Wavenumber-Frequency Spectrum Beneath a Turbulent Boundary Layer Measured With Transducer Arrays Calibrated With an Acoustical Method," ASME Winter Annual Meeting, NCA-Vol. 11/FED-Vol. 130, pp. 21-35.

Panton, R. L., and Linebarger, J. H., 1974, "Wall Pressure Spectra Calculations for Equilibrium Boundary Layers," *Journal of Fluid Mechanics*, Vol. 65, pp. 261-287.

Panton, R. L., Goldman, A. L., Lowery, R. L., and Reischman, M. M., 1980, "Low-Frequency Pressure Fluctuations in Axisymmetric Turbulent Boundary Layers," *Journal of Fluid Mechanics*, Vol. 97, Part 2, pp. 299-319.

Panton, R. L., 1990, "Inner-Outer Structure of Wall-Pressure Correlation Function," Kline and Afgan, *Near Wall Turbulence*, pp. 381-396.

Roberts, Gilles, 1993, "The Wall-Pressure Spectrum Under a Turbulent Boundary Layer: Part 1, Experiments," ASME Winter Annual Meeting, FED-Vol. 155, pp. 37-43.

Wilczynski, V., and Casarella, M. J., 1993, "The Relationship Between Organized Structures and Wall Pressure Fluctuations," ASME Winter Annual Meeting, NCA-Vol. 11/FED-Vol. 150, pp. 59.

Willmarth, W. W., 1975, "Pressure Fluctuations Beneath Turbulent Boundary Layers," *Annual Review of Fluid Mechanics*, Vol. 7, pp. 13-38.

Willmarth, W. W., and Yang, C. S. 1970, "Wall-Pressure Fluctuations Beneath Turbulent Boundary Layers on a Flat Plate and a Cylinder," *Journal of Fluid Mechanics*, Vol. 11, Part 1, pp. 47-80.

Wills, J. A. B., 1970, "Measurements of the Wave-Number/Phase Velocity Spectrum of Wall Pressure Beneath a Turbulent Boundary Layer," *Journal of Fluid Mechanics*, Vol. 45, Part 1, pp. 65-90.